Available online at www.sciencedirect.com
SCIENCE DIRECT®
Journal of Non-Crystalline Solids 351 (2005) 2493–2500
JOURNAL OF NON-CRYSTALLINE SOLIDS
www.elsevier.com/locate/jnoncrysol

Structural and magnetic properties of MoO_3–TeO_2 glasses

A. Mekki [a], G.D. Khattak [a], L.E. Wenger [b,*]

[a] Department of Physics, King Fahd University of Petroleum and Minerals, Dhahran 31261, Saudi Arabia
[b] Department of Physics, The University of Alabama at Birmingham, CH 464, 1530 3rd Avenue S, Birmingham, AL 35294, USA

Received 7 March 2005; received in revised form 13 May 2005

Abstract

A series of tellurite glasses containing MoO_3 with the nominal composition $x(MoO_3)$–$(1-x)(TeO_2)$, where $x = 0.10$, 0.20, 0.30, and 0.40, have been investigated using X-ray photoelectron spectroscopy (XPS) and temperature-dependent magnetization techniques. The Te 3d core level spectra for all glass samples show symmetrical peaks at essentially the same binding energies as measured for TeO_2 oxide and with full-widths at half-maximum (FWHM) that do not vary with increasing MoO_3. These features indicate that the chemical environment of the Te atoms in the glasses does not vary significantly with the addition of MoO_3 and that the Te ions exist in a single configuration, namely TeO_4 trigonal bipyramid (tbp). The O 1s spectra, however, show asymmetry for samples with composition $x \leqslant 0.30$ and are subsequently fitted with two peaks. One arises from the presence of oxygen atoms in the Te–O–Te, Mo–O–Mo and Te–O–Mo environments which are termed bridging oxygen (BO) and the other from oxygen atoms in an Mo=O environment which are termed non-bridging oxygen (NBO). The O 1s peak for $x = 0.40$ is more narrow and symmetric, and is fitted to a single peak due to the BO atoms. While the analysis of the Mo 3d spectra indicates the presence of Mo^{6+} ions only, the temperature-dependent magnetic susceptibility measurements shows a weak paramagnetic behavior which can be explained by having less than 1 at.% of the Mo ions existing in a magnetic Mo^{5+} valence state, a percentage below the detection level of the XPS determinations.

PACS: 61.14.Qp; 61.43.Fs; 75.20.−g

1. Introduction

Binary tellurite glasses are of interest to glass scientists and technologists due to their wide range of technological applications such as memory switching devices and gas sensors [1,2]. TeO_2 is of particular interest as this conditional glass network former has a low melting point and can form a glass when combined with alkali metal ions, transition metal ions, and even rare earth ions [3–5]. The formation of these glasses may also be accompanied by a change in the local TeO_2 structure from the three-dimensional network of TeO_4 trigonal bipyramid (tbp) structural units. For example, the addition of alkali metal ions in tellurite glasses results in the transformation of some TeO_4 units in the glass network into TeO_3 trigonal pyramid (tp) with non-bridging oxygen [6]. Similar transformations of the TeO_4 structural unit to the TeO_3 unit are found with increasing V_2O_5 content in V_2O_5–TeO_2 glasses and with increasing WO_3 content in WO_3–TeO_2 glasses [7,8]. Thus studies of the glass structure and its corresponding effect on the electronic properties continue to be investigated by a multitude of techniques.

Similarly, the electrical and structural properties of Mo–Te glasses have also been previously investigated by several groups using spectroscopic techniques, although with some differences in the structural determinations [9–11]. In a systematic structural study by

* Corresponding author. Tel.: +1 205 934 5102; fax: +1 205 975 6111.
E-mail address: wenger@uab.edu (L.E. Wenger).

0022-3093/$ - see front matter © 2005 Elsevier B.V. All rights reserved.
doi:10.1016/j.jnoncrysol.2005.06.025

Raman spectroscopy, Sekiya et al. [9] found that the basic structural units in $x\mathrm{MoO_3}$–$(1-x)\mathrm{TeO_2}$ are $\mathrm{TeO_4}$ tbp, $\mathrm{TeO_{3+1}}$ polyhedra, and $\mathrm{MoO_6}$ octahedra with no $\mathrm{TeO_3}$ tp units. Moreover, their results suggest that the number of Mo=O bonds in each $\mathrm{MoO_6}$ octahedra decreases from two for low $\mathrm{MoO_3}$ content to one when the $\mathrm{MoO_3}$ content exceeds 30%. On the other hand, Dimitriev et al. report that the basic structural units of these binary tellurite glasses are $\mathrm{TeO_4}$ tbp and $\mathrm{Mo_2O_8}$ groups (one Mo=O bond per Mo ion) for $x < 0.40$, while the glass structure for higher Mo content consists of $\mathrm{MoO_6}$ octahedra with some $\mathrm{TeO_4}$ being transformed into $\mathrm{TeO_3}$ units [11]. A more recent study suggested the presence of $\mathrm{MoO_4}$, $\mathrm{MoO_6}$, $\mathrm{TeO_4}$, and $\mathrm{TeO_3}$ structural units for all glass compositions ranging from 0.30 to 0.70 $\mathrm{MoO_3}$ [10]. Moreover, this study reported that $\mathrm{Mo^{4+}}$, $\mathrm{Mo^{5+}}$, and $\mathrm{Mo^{6+}}$ ions exist simultaneously in these glasses. In light of the differing results from these previous studies we have investigated this glass system and its structure by X-ray photoelectron spectroscopy (XPS) and magnetization techniques. XPS has proven to be an important and useful technique not only in assessing the local glass structure as it can distinguish between bridging oxygen (BO) and non-bridging oxygen (NBO) [12], but also in estimating the ratio of the different valence states in the TM-oxide glasses [13–15]. In this study, XPS is used to investigate the role of Mo ions in the Mo–Te glasses, the oxidation state of Mo ions as well as to study the local glass structure, specifically to investigate the possibility of transformation of $\mathrm{TeO_4}$ units into $\mathrm{TeO_3}$ units at high $\mathrm{MoO_3}$ content. Temperature-dependent magnetic susceptibility measurements combined with inductively coupled plasma spectroscopy (ICP) provide an independent measure of the relative amounts of the different Mo valence states in these glasses. This study is also part of our continuing study of transition metal-doped tellurite glasses. In previous work on the Cu-tellurite glass system, CuO entered the glass network as a glass modifier introducing non-bridging oxygen sites proportional to the Cu content (10–40 mol%) while the Te ions remained in the $\mathrm{TeO_4}$ tbp structure with negligible $\mathrm{TeO_3}$ being formed [4].

2. Experimental details

2.1. Sample preparation

All glasses were prepared by melting dry mixtures of reagent grade $\mathrm{MoO_3}$ and $\mathrm{TeO_2}$ in alumina crucibles to form nominal $x(\mathrm{MoO_3})$–$(1-x)(\mathrm{TeO_2})$ compositions with $x = 0.10$, 0.20, 0.30, and 0.40. Since oxidation and reduction reactions in a glass melt are known to depend on the size of the melt, the sample geometry, whether the melt is static or stirred, thermal history, and quenching rate, all glass samples were prepared under similar conditions to minimize these factors. Approximately 30 g of chemicals were thoroughly mixed in an alumina crucible to obtain a homogenized mixture for each $\mathrm{MoO_3}$ concentration. The crucible containing the nominal mixture was then transferred to a furnace maintained at 900–950 °C. The melt was left for about an hour under atmospheric conditions in the furnace during which the melt was occasionally stirred with an alumina rod. The homogenized melt was then cast onto a stainless steel plate mold to form glass rods of approximately 5 mm diameter and 2 cm in length for XPS measurements. After casting, the specimens were annealed at 200 °C for 10 h and were stored in a vacuum dessicator to minimize any further oxidation of the glass samples. The amorphous nature of these glasses was confirmed by the absence of any peaks in the X-ray diffraction spectra. The actual compositions of the glasses were determined by inductively coupled plasma spectroscopy (ICP) and are listed in Table 1. Although the inclusion of alumina from the crucibles used in the melting of the glass mixtures can be a possible source of impurities, no signals for aluminum were detected in either the XPS or ICP measurements on these glasses.

2.2. XPS measurements

Core level photoelectron spectra were collected on a VG scientific ESCALAB MKII spectrometer equipped with a dual aluminum-magnesium anode X-ray gun and a 150-mm concentric hemispherical analyzer using $\mathrm{Al\,K_\alpha}$ ($h\upsilon = 1486.6$ eV) radiation from an anode operated at 130 W. Photoelectron spectra of the Te 3d, Mo 3d, and O 1s core levels were recorded using a computer-controlled data collection system with the electron analyzer set at a pass-energy of 20 eV for the high-resolution scans. The energy scale of the spectrometer was calibrated using the core level of Cu $2p_{3/2}$ (=932.67 eV), Cu $3p_{3/2}$ (=74.9 eV), and Au $4f_{7/2}$ (=83.98 eV) photoelectron lines. For self-consistency, the C 1s transition at 284.6 eV was used as a reference for all charge shift corrections as this peak arises from hydrocarbon contamination and its binding energy is generally accepted as remaining constant, irrespective of the chemical state of the sample. For XPS measure-

Table 1
Nominal and actual composition (molar fraction) of various molybdenum tellurite glasses

Nominal		Actual (from ICP)	
$\mathrm{MoO_3}$	TeO2	$\mathrm{MoO_3}$	$\mathrm{TeO_2}$
0.10	0.90	0.092	0.908
0.20	0.80	0.185	0.815
0.30	0.70	0.281	0.719
0.40	0.60	0.353	0.647

The uncertainty in the ICP results is ±5%.

ments, a glass rod from each composition was cleaved in the preparation chamber at a base pressure of 2×10^{-9} mbar before being transferred to the analysis chamber where the pressure was maintained at $<2 \times 10^{-10}$ mbar. A period of approximately 2 h was required to collect the spectral data set for each sample. A non-linear, least-squares algorithm was employed to determine the best fit of each O 1s, Mo 3d, and Te 3d spin–orbit doublet spectrum to two Gaussian–Lorentzian curves in order to represent bridging and non-bridging oxygen sites, two possible Mo oxidation states (Mo^{5+} and Mo^{6+}), and tbp and tp Te structural units, respectively. The fraction of non-bridging oxygen, Mo^{6+}, and tbp units were determined from their respective area ratios from these fits. Based on the reproducibility of similar quantitative spectral decompositions of spectra taken from other surfaces on the same glass samples, uncertainties of ±5% for NBO content and ±10% for both Mo^{6+} and TeO_4 units were estimated for these area ratios.

2.3. Magnetic measurements

The temperature-dependent dc magnetic susceptibility was measured using a SQUID magnetometer (Quantum Design model MPMS-5S) in a magnetic field of 5000 Oe over a temperature range 5–300 K at temperature intervals of 2.5 K. The susceptibility of the sample holder is negligible below 100 K for all samples and constitutes less than a 2% correction at the highest temperature for all samples. The overall accuracy of the magnetic measurements is estimated to be approximately 3% due to the uncertainty of the magnetometer calibration.

3. Results

3.1. Te 3d spectra

The Te 3d core level spectra for all Mo–Te glasses are collectively displayed in Fig. 1. The doublet peaks attributed to the Te $3d_{5/2}$ and Te $3d_{3/2}$ transitions in these spectra have essentially the same binding energies (BE) for all glass compositions with the BE of the Te $3d_{5/2}$ transition being ~576 eV with an energy separation between the Te $3d_{5/2}$ and Te $3d_{3/2}$ peaks of ~10.4 eV. While the intensities of these peaks decrease with increasing Mo content as expected, the peaks remain symmetric with a full-width at half-maximum (FWHM) of ~2.6 to 2.3 eV as indicated in Table 2. Similar values of 576.1, 2.1, and 10.4 eV were found for the BE, FWHM, and spin–orbit peak separation from the Te 3d spectra for TeO_2.

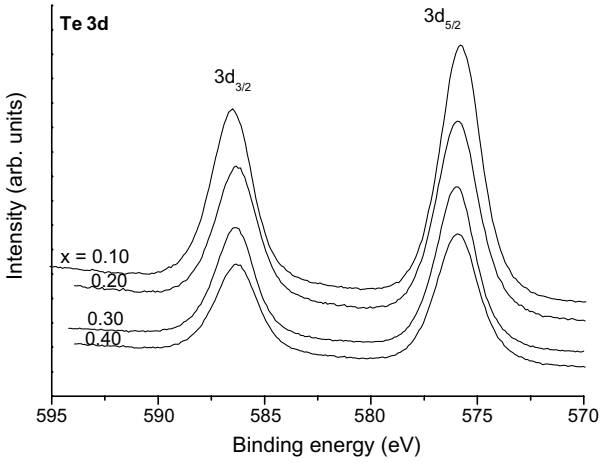

Fig. 1. Core level Te 3d spectra for the $x(MoO_3)$–$(1-x)(TeO_2)$ glasses.

3.2. O 1s spectra

Fig. 2 shows the O 1s core level spectra for all glasses investigated in this study. While the O 1s peaks have essentially the same BE for all glass compositions (see Table 2), the peaks for the $x \leqslant 0.30$ are considerably broader than that for the $x = 0.40$ as evidenced by the larger FWHM values. In fact, this broadness may be attributable to an asymmetry in the peak resulting from the appearance of a shoulder on the lower BE side of the peak, which is most clearly evident in the spectrum for the glass with 0.30 MoO_3 content. Since any asymmetry in the O 1s spectrum would indicate the existence of

Table 2
Peak positions in eV for the core levels Te $3d_{5/2}$, Mo $3d_{5/2}$, and O 1s relative to C 1s (284.6 eV), their corresponding FWHM (full-width at half-maximum), and the separation ΔE of the spin–orbit peaks

x	Te $3d_{5/2}$	FWHM	ΔE(Te 3d)	Mo $3d_{5/2}$	FWHM	ΔE(Mo 3d)	O 1s	FWHM
0.10	576.0	2.6	10.5	232.5	2.4	3.1	530.6[a]	2.2
0.20	575.9	2.6	10.4	232.6	2.3	3.2	530.6[a]	2.3
0.30	576.0	2.6	10.4	232.6	2.4	3.2	530.6[a]	2.4
0.40	576.1	2.3	10.4	232.6	2.4	3.2	530.6[a]	2.0
TeO_2	576.1	2.1	10.4					
MoO_3				232.6		3.1		

The uncertainty in the peak position is ±0.1 eV and in FWHM is ±0.2 eV.
[a] These peak positions are the average of two peaks.

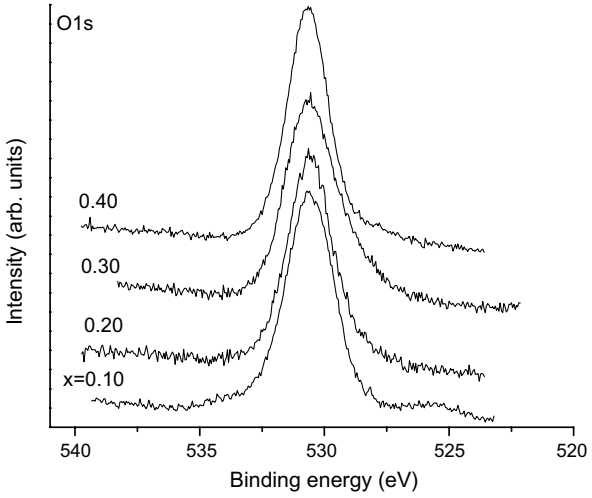

Fig. 2. Core level O 1s spectra for the $x(MoO_3)$–$(1-x)(TeO_2)$ glasses.

more than one type of oxygen sites in these glasses, all O 1s spectra were fitted to two Gaussian–Lorentzian peaks in order to determine the peak positions and relative abundance of two different oxygen sites.

3.3. Mo 3d spectra

The Mo 3d spin–orbit doublet spectra for the glasses are shown in Fig. 3. One first notes that the intensities of these Mo 3d peaks grow with increasing MoO_3 content as expected. The BE of the maximum peak intensity for the two spin–orbit components, Mo $3d_{5/2}$ and Mo $3d_{3/2}$, are ~232 eV and ~235 eV, respectively, an energy separation of 3.1 eV for all glass compositions. These components also appear to be symmetric with FWHM of ~2.4 eV for both components (see Table 2).

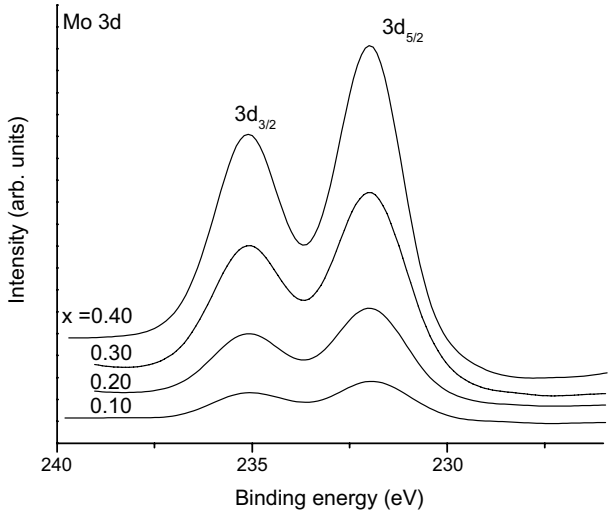

Fig. 3. Core level Mo 3d spectra for the $x(MoO_3)$–$(1-x)(TeO_2)$ glasses.

3.4. Temperature dependent magnetization

The magnetic susceptibility results for these glasses are displayed in Fig. 4 as plots of the magnetic susceptibility, M/H, as a function of the temperature T. The susceptibility data for all samples appear to follow a Curie–Weiss behavior ($M/H = C/(T-\theta)$) on top of a negative temperature-independent contribution arising from the ion core diamagnetism. The temperature-independent constant for each glass sample was determined from a high-temperature extrapolation of M/H vs $1/T$ plots for temperatures above 200 K. After subtracting these temperature-independent constants from the measured susceptibility data, the resulting M^*/H ($=M/H-(M/$

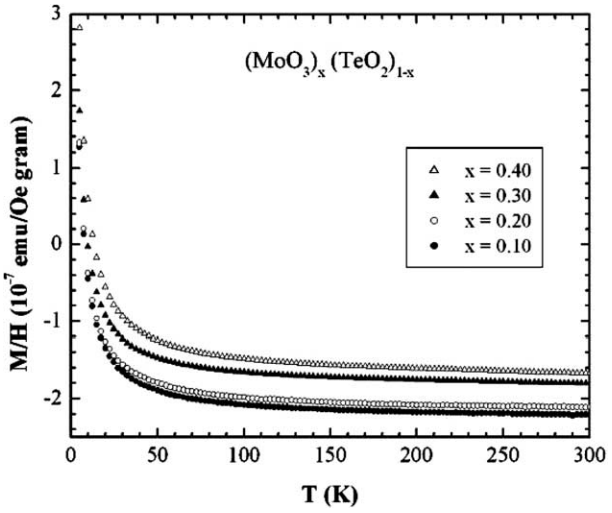

Fig. 4. Magnetic susceptibility-versus-temperature for the $x(MoO_3)$–$(1-x)(TeO_2)$ glasses.

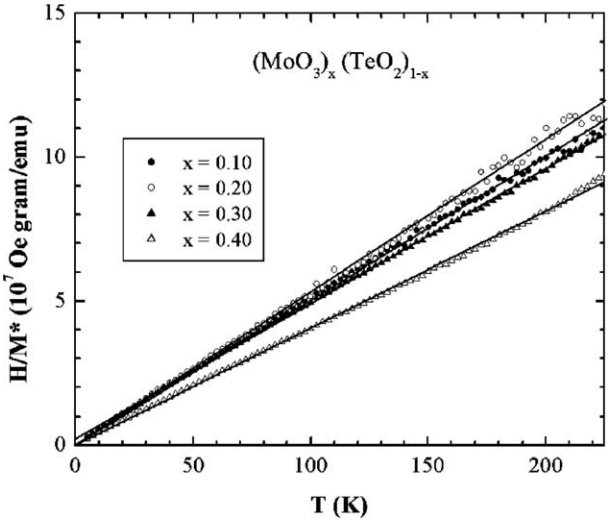

Fig. 5. The inverse of the 'corrected' magnetic susceptibility ($M^*/H = M/H - (M/H)_{constant}$) as a function of temperature for the MoO_3-tellurite glasses.

Table 3
Magnetic susceptibility results for the $x\mathrm{MoO_3}$–$(1-x)(\mathrm{TeO_2})$ glass samples and the concentration of Mo^{5+} ions to total Mo ions

x	$(M/H)_{\mathrm{constant}}$ (10^{-7} emu/Oe g)	C (10^{-6} emu K/Oe g)	θ (K)	$(Mo^{5+}/Mo_{\mathrm{total}})$
0.10	−2.28	1.99	−1.82	0.009
0.20	−2.18	1.90	−0.71	0.004
0.30	−1.86	2.17	−7.48	0.003
0.40	−1.73	2.52	−1.76	0.003

$H)_{\mathrm{constant}}$) data follow a Curie–Weiss behavior ($=C/(T-\theta)$) as shown in Fig. 5. The resulting parameters – $(M/H)_{\mathrm{constant}}$, the Curie constant C, and the paramagnetic Curie temperature θ – obtained from a least-squares fitting procedure are listed in Table 3 for all compositions.

4. Discussion

As seen from Table 2, the values of the BE, FWHM, and spin–orbit peak separation of the Te 3d core level spectra for the Mo–Te glass samples are very comparable to the values for TeO_2, although the FWHM values are slightly larger. This would suggest that the predominant structural units are TeO_4 trigonal bipyramids. However, structural units of the TeO_{3+1} type as suggested by Sekiya et al. cannot be excluded as these structural units would probably be indistinguishable in the spectra due to the energy resolution of our spectrometer being ~1.0 eV, and thus could give rise to the broader peaks in our observations [9]. On the other hand, the BE of Te $3d_{5/2}$ from TeO_3 structural units is ~573 eV, which is within the energy resolution of our spectrometer [16]. Therefore, if TeO_3 units are present in these glasses, they should be easily observed as a separate contribution to the Te 3d spectra. In order to confirm the non-existence of the TeO_3 structural units in our glasses, fits of the Te $3d_{5/2}$ spectra to two contributions, one due to TeO_4 units at a BE of 576 eV and the other due TeO_3 units at a BE of 573 eV, were attempted. In all four spectra the fitting software converges to a single peak at 576 eV with a FWHM of ~2.6 eV. Fig. 6 shows the resultant fitting of the Te 3d spin–orbit doublet for the $x = 0.10$ glass composition. If the TeO_3 units exist in these glasses, their abundance is below the detection limit which is estimated to be 2%.

Since any asymmetry in the O 1s peak is indicative of at least two oxygen different oxygen sites, each O 1s spectrum was fitted to two Gaussian–Lorentzian peaks as shown in Fig. 7(a) for the $x = 0.20$ composition glass. However, the O 1s spectrum for the $x = 0.40$ composition glass (see Fig. 7(b)) was satisfactorily fitted to a single Gaussian–Lorentzian peak with a smaller FWHM. The numerical results of these fits are also displayed in Table 4 in terms of the contributions arising from a higher BE site of 530.6 eV (designated as BO) and a lower BE site of 529.1 eV (designated as NBO). In order to quantify the relative abundance of these two sites in each glass, the ratios of the area under the NBO peak to the total peak area were determined from the fits and are also shown in Table 4. It is clear from Table 4 that the ratio NBO/TO increases nearly linear with MoO_3 concentration for $x \leqslant 0.30$, then becomes zero for $x = 0.40$ as only BO-type sites are present. Based on other structural studies, it is reasonable to assume that the NBO-type site consists of oxygen associated with Mo=O bonds in the MoO_6 octahedral structures and the BO-type sites with oxygen in Te–O–Te, Mo–O–Mo, and Te–O–Mo bonds [9–11]. It is reasonable to assume that the BE of these three BO-type sites will be essentially the same as the electronegativities of Te and Mo are nearly identical, 2.1 and 2.16, respectively. Moreover, a larger electron density can be expected at

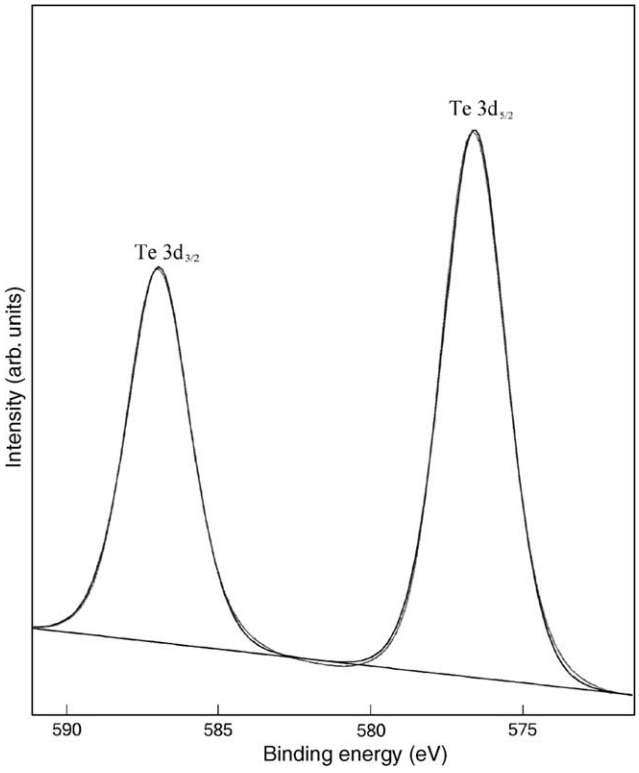

Fig. 6. The Te 3d spectrum for the $x = 0.10$ MoO_3 tellurite glass sample and the resultant least-squares fit to a single Gaussian–Lorentzian peak.

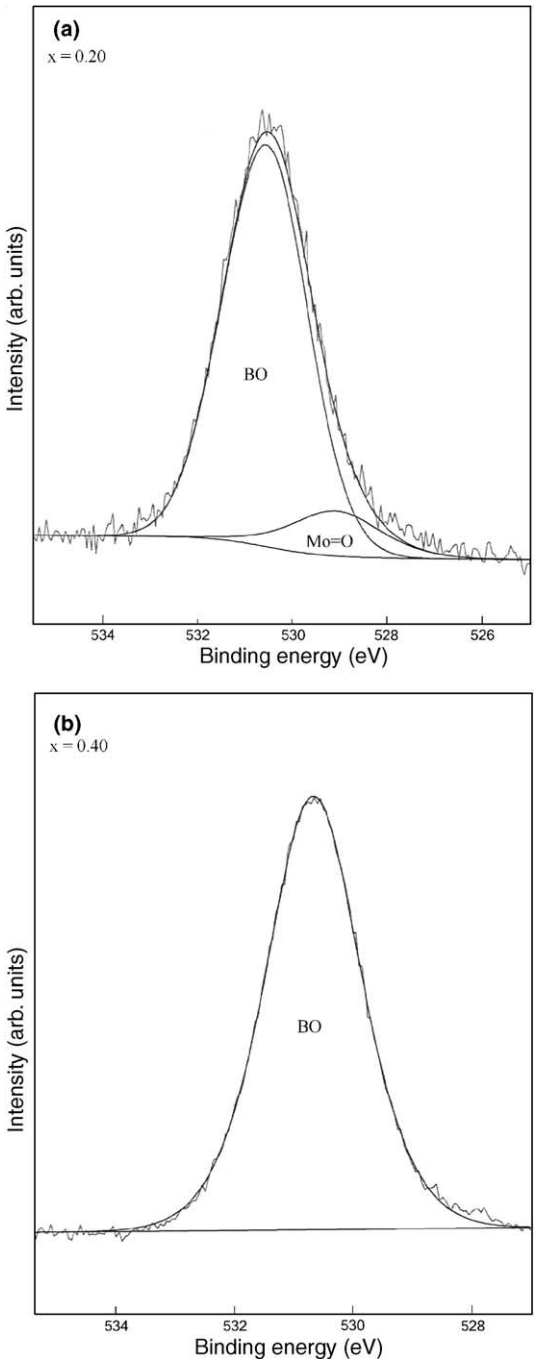

Fig. 7. The O 1s spectra for the (a) $x = 0.10$ and (b) 0.40 MoO_3 tellurite glass samples and the resulting NBO and BO peaks (dashed lines) from the least-squares fitting routine to two Gaussian–Lorentzian peaks. The smooth solid line is the resultant sum of the two peaks.

the O site for the Mo=O configuration than for the other two configurations which results in a lower BE peak for the Mo=O configuration. With two Mo=O sites in each MoO_6 octahedra, the ratio of NBO/TO is given by

$$\frac{\mathrm{NBO}}{\mathrm{TO}} = \frac{2x}{3x + 2(1-x)} = \frac{2x}{2+x}. \quad (1)$$

Table 4
Peak positions, FWHM, and relative concentration of NBO resulting from the curve fitting of the O 1s core level for the $x\mathrm{MoO_3}$–$(1-x)(\mathrm{TeO_2})$ glasses

x	O 1s (eV)		FWHM (eV)		[NBO]/[TO]	
	NBO	BO	NBO	BO	Measured	Eq. (1)
0.10	529.1	530.6	2.3	2.1	0.10	0.09
0.20	529.2	530.6	2.5	2.1	0.18	0.17
0.30	529.1	530.6	2.5	2.1	0.26	0.25
0.40		530.6		2.0	0.00	0.30

The numerical results based on Eq. (1) are in reasonably good quantitative agreement with the experimental determinations for the $x \leqslant 0.30$ glasses as seen in Table 4. However, this result is neither consistent with the hypothesis from Ref. [9] that the number of Mo=O bonds decreases from two-to-one with increasing Mo concentration nor the conclusion that there are two unshared oxygen atoms per Mo_2O_8 group [11]. Moreover, the observation that only a single peak at the BE of the BO-type site can be fitted to the $x = 0.4$ glass spectrum (NBO/TO = 0) indicates that either there are no Mo=O configurations or that the BE of the Mo=O shifts to a higher energy for $x > 0.3$ and is indistinguishable from the BO atoms. The former conjecture would require essentially all MoO_6 octahedra to have no Mo=O bonds as the absence of any shift in the Mo $3d_{5/2}$ peak indicates no change in the local environment surrounding the Mo ion. Alternatively, one expects at MoO_3 concentrations greater than 33% that the local glass structure will resemble $MoTe_2O_7$, which has one Mo=O configuration. Thus the latter conjecture can not be completely ruled out.

Since molybdenum ions can exist in more than one oxidation state, each of the Mo $3d_{5/2}$ spectra was fitted to two contributions, one due Mo^{6+} ions at a BE of 232.5 eV and the other at a BE of 230 eV due to Mo^{5+} ions [10]. However, the fitting software would always converge to a single peak at a BE of 232.5 eV. Fig. 8 shows such a fitting for the $x = 0.20$ glass composition with the relevant fitting data displayed in Table 2. Since no resolvable peak is observed at 229 eV (BE of Mo^{4+}) in any of the Mo 3d spectra, one can also conclude that there is no Mo^{4+} present either. This suggests that the only oxidation state of the Mo ions in these glasses is 6+.

As described previously, the best fit to the magnetic susceptibility data was found to consist of a negative temperature-independent term plus a Curie–Weiss-like temperature-dependent behavior. The temperature-independent term can be understood in terms of two contributions: a diamagnetic one arising from the core ions in the glass matrix, and a temperature-independent paramagnetic contribution arising from the presence of MoO_3 in the tellurite glasses (-42×10^{-6} $\mathrm{cm^3/mol}$

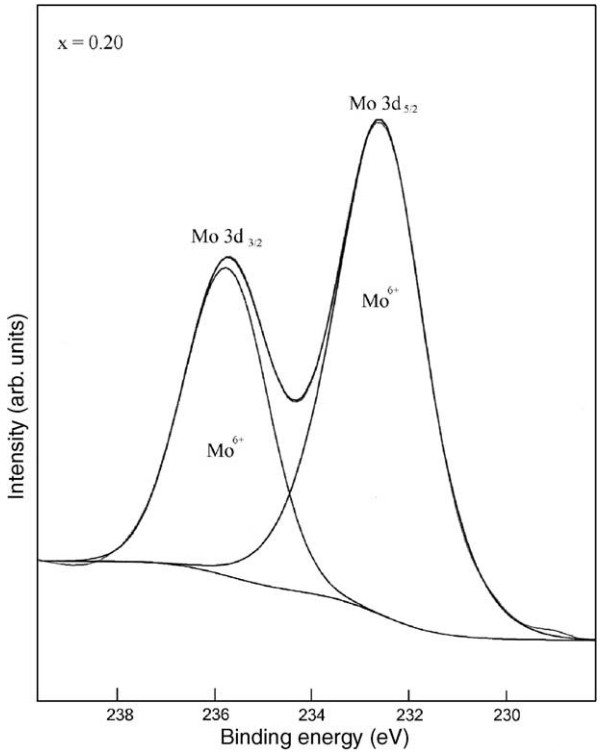

Fig. 8. The Mo 3d spectrum for the $x = 0.20$ MoO_3 tellurite glass samples and the resultant least-squares fit to a single Gaussian–Lorentzian peak.

TeO_2 and 3×10^{-6} cm^3/mol MoO_3) [17,18]. Using the actual molar content from Table 1, values ranging from -3.8 to -2.6×10^{-6} cm^3/mol are estimated for the temperature-independent term which are in reasonable agreement to the experimental values (-3.6 to -2.7×10^{-6} cm^3/mol). Moreover, the decrease in the negative $(M/H)_{\text{constant}}$ values with increasing MoO_3 content is consistent with the temperature-independent paramagnetic MoO_3 contribution increasing with increasing MoO_3 content. On the other hand, the Curie temperature-dependent behavior observed in these glasses must be associated with a fraction of the molybdenum ions being in another oxidation state other than Mo^{6+} since Mo^{6+} ions are non-magnetic. The most probable oxidation state is Mo^{5+} which has a magnetic moment, $p_{\text{eff}} = 1.73\mu_B$. Thus, from the Curie constant C in conjunction with the molybdenum concentration determined by chemical analysis on these oxide glasses, 0.3–0.9% of the total Mo concentration for these glasses would have to be in the Mo^{5+} state as shown in Table 3. These very low percentages are below the detection level of the XPS determinations and correspondingly do not have an effect on the conclusions of the local structure of this tellurite glass system. The negative paramagnetic Curie temperature values in the range of -0.7 to -7.5 K indicate a weak antiferromagnetic interaction between the Mo^{5+} ions. These small values are not surprising since θ is proportional to the number of neighboring magnetic ions as well as the strength of the magnetic interaction.

5. Conclusion

The basic structural units of the binary MoO_3–TeO_2 glasses synthesized by a melt-quenching technique are found to be consistent with the presence of MoO_6 octahedra and TeO_4 tbp structures only and no TeO_3 tp units. The O 1s core level spectra indicates bridging oxygen atoms in Te–O–Te, Te–O–Mo and Mo–O–Mo configurations at a slightly higher binding energy than the non-bridging oxygen atoms in the Mo=O configuration with the proportion of NBO's increasing linearly with MoO_3 content for $x \leqslant 0.3$. For the 0.40 MoO_3 glass sample, all oxygen atoms have the BE of the BO atoms. The analyses of the Mo 3d spectra indicate the existence of only Mo ions in the 6+ oxidation state for all compositions, which is also consistent with the analysis of the magnetic susceptibility measurements on the same samples.

Acknowledgements

Two of the authors (A. Mekki and G.D. Khattak) would like to acknowledge the support of KFUPM. This work was supported by the Research Committee at KFUPM under Grant No. SAB/2004/04.

References

[1] H. Hirashima, H. Ide, T. Yoshida, J. Non-Cryst. Solids 86 (1986) 327.
[2] S. Chakraborty, H. Satou, H. Sakata, J. Appl. Phys. 82 (1997) 5520.
[3] Y. Himei, Y. Miura, T. Nanba, A. Osaka, J. Non-Cryst. Solids 211 (1997) 64.
[4] G.D. Khattak, A. Mekki, L.E. Wenger, J. Non-Cryst. Solids 337 (2004) 174.
[5] R.A. El Mallawany, G.A. Saunders, J. Mater. Science Lett. 7 (1988) 870.
[6] Y. Himei, A. Osaka, T. Namba, Y. Miura, J. Non-Cryst. Solids 177 (1995) 164.
[7] Y. Dimitriev, V. Dimitrov, Mater. Res. Bull. 13 (1978) 1071.
[8] P. Charton, L. Gengember, P. Armand, J. Solid State Chem. 168 (2002) 175.
[9] T. Sekiya, N. Mochida, S. Ogawa, J. Non-Cryst. Solids 185 (1995) 135.
[10] M. Pal, K. Hirota, Y. Tsujigami, H. Sakata, J. Phys. D 34 (2001) 459.
[11] Y. Dimitriev, V. Dimitrov, M. Arnaudov, J. Mater. Sci. 18 (1983) 1353.
[12] R. Bruckner, H.U. Chun, H. Goretski, M. Sammet, J. Non-Cryst. Solids 42 (1980) 49.
[13] A. Mekki, G.D. Khattak, L.E. Wenger, J. Non-Cryst. Solids 330 (2003) 156.
[14] A. Mekki, G.D. Khattak, D. Holland, M. Chinkhota, L.E. Wenger, J. Non-Cryst. Solids 318 (2003) 193.

[15] A. Mekki, D. Holland, K.A. Ziq, C.F. McConville, J. Non-Cryst. Solids 272 (2000) 179.
[16] B.V.R. Chowdari, K.L. Tan, F. Ling, Solid State Ionics 113–118 (1998) 711.
[17] P.W. Selwood, Introduction to Magnetochemistry, Interscience, NY, 1956.
[18] J. Baudet, J. Chim. Phys. 58 (1961) 853.